Hindawi
Shock and Vibration
Volume 2021, Article ID 6673965, 19 pages
https://doi.org/10.1155/2021/6673965

Research Article

A Fault Feature Extraction Method for Rolling Bearing Based on Intrinsic Time-Scale Decomposition and AR Minimum Entropy Deconvolution

Jiakai Ding,[1,2] Liangpei Huang,[1] Dongming Xiao ,[1,2] and Lingli Jiang[2]

[1]*Hunan Provincial Key Laboratory of Health Maintenance for Mechanical Equipment, Hunan University of Science and Technology, Xiangtan 411201, China*
[2]*School of Mechatronics Engineering, Foshan University, Foshan 528225, China*

Correspondence should be addressed to Dongming Xiao; dongming.xiao@outlook.com

Received 11 November 2020; Revised 30 December 2020; Accepted 2 January 2021; Published 13 January 2021

Academic Editor: Liang Guo

It is very difficult to extract the feature frequency of the vibration signal of the rolling bearing early weak fault and in order to extract its feature frequency quickly and accurately. A method of extracting early weak fault vibration signal feature frequency of the rolling bearing by intrinsic time-scale decomposition (ITD) and autoregression (AR) minimum entropy deconvolution (MED) is proposed in this paper. Firstly, the original early weak fault vibration signal of the rolling bearing is decomposed by the ITD algorithm to proper rotations (PRs) with fault feature frequency. Then, the sample entropy value of each PR is calculated to find the largest PRs of the sample entropy. Finally, the AR-MED filtering algorithm is utilized to filter and reduce the noise of the largest PRs of the sample entropy value, and the early weak fault vibration signal feature frequency of the rolling bearing is accurately extracted. The results show that the ITD-AR-MED method can extract the early weak fault vibration signal feature frequency of the rolling bearing accurately.

1. Introduction

Rolling bearings play a pivotal role in modern industry and their applications are very extensive, such as aircraft engines [1, 2], gas turbines [3], landing gear [4], flexible mechanism [5], and wind turbines [6–11]. However, the rolling bearing is very easy to cause damage in a strong vibration environment, and the rolling bearing is very prone to failure in most rotating machinery systems. The failure of the rolling bearing will even cause a catastrophic accident to the rotating machinery system, which will indirectly cause huge economic losses. Therefore, it is significant to accurately extract the early weak fault vibration signal feature frequency of the rolling bearing [12].

At present, vibration signal [13–15] is mostly used for rolling bearing fault diagnosis analysis. Because the rolling bearing usually works in complex environmental noise, and the collected fault vibration signal feature frequency of the rolling bearing is usually weak [16, 17]. Many researchers use the signal decomposition algorithms such as empirical mode decomposition (EMD) [18, 19], wavelet packet decomposition (WPT) [20–22], and local mode decomposition (LMD) [23–25] to reduce the noise of the original signal. However, the wavelet basis function (WBF) is fixed before the WPT decomposition and the decomposition effect according to the selection of the WBF. Therefore, WPT has obvious defects in vibration signal decomposition. The EMD and LMD are prone to adverse factors such as endpoint effects and mode mixing [26–29]. Therefore, Frei and Osorio [30] proposed an intrinsic time-scale decomposition (ITD) adaptive signal decomposition algorithm. The ITD algorithm can effectively solve the unfavorable factors between EMD and LMD. Xing et al. [31] developed the ITD method combined with singular value decomposition (SVD) and support vector machine (SVM) method. The original vibration signal is decomposed by the ITD algorithm, and the

proper rotations (PRs) with the greatest correlation was selected for subsequent analysis. An [32] utilized the ITD algorithm in fault diagnosis under four fault states collected. The first few PRs were selected for spectral analysis to find out their feature frequency. Feng et al. [33] utilized the ITD algorithm in fault diagnosis and feature extraction of the planetary gearbox.

The fault vibration signal of the rolling bearing usually presents the characteristics of the impact waveform [34] when the rolling bearing fails. Wiggins [35] proposed a minimum entropy deconvolution (MED) filtering method to enhance the impact component in the fault vibration signal. This method can enhance the impact component and the fault feature in the signal. Sawalhi et al. [36] and Endo and Randall [37] utilized the MED to enhance the impact component of the rolling bearing and gear vibration signal, respectively, and the experiment results proved that this method could effectively enhance the feature frequency. Jiang et al. [38] proposed a condition monitoring method of the rolling bearing based on the MED and envelope spectrum. After the rolling bearing fault vibration signal was filtered by the MED, its fault feature frequency was enhanced, and then an envelope spectrum analysis was performed on it; thus, the rolling bearing fault feature frequency was separated accurately. Li et al. [39] developed an autoregression (AR) MED and variational mode decomposition (VMD) fault diagnosis method. Among them, the AR-MED method can eliminate the influence of background noise effectively, which can enhance the feature frequency in the fault signal.

In summary, this paper studied the problem of extracting early weak fault vibration signal feature frequency of the rolling bearing under complex background noise. This paper proposes a method for extracting early weak fault vibration signal feature frequency of the rolling bearing based on ITD and AR-MED.

2. ITD Signal Decomposition Method

Suppose that the original signal X_t to be decomposed is a real value discrete signal, ξ is defined as the baseline extraction factor of X_t, $H_t = X_t - \xi X_t$ is defined as the proper rotations (PRs), where ξX_t is the mean curve of the signal, denoted as $L_t = \xi X_t$; then, the primary decomposition of the original signal can be expressed as

$$X_t = L_t + H_t. \tag{1}$$

Then, the steps of the ITD algorithm are as follows:

(1) Extract the extreme point X_k of X_t and the corresponding time point τ_k. Among them, $k = 1, 2, \ldots, N$ and definition $\tau_0 = 0$, so definition L_{k+1} is

$$L_{k+1} = \alpha\left[X_k + \left(\frac{\tau_{k+1} - \tau_k}{\tau_{k+2} - \tau_k}\right)\left(X_{k+2} - X_k\right)\right] + (1 - \alpha)X_{k+1}, \tag{2}$$

where $\alpha \in [0, 1]$, $\alpha = 0.5$, and $k = 1, 2, \ldots, N - 2$.

(2) The piecewise linear baseline extraction factor of signal X_t is defined as

$$L_t = \xi X_t = L_k + \left(\frac{L_{k+1} - L_k}{X_{k+1} - X_k}\right)(X_t - X_k). \tag{3}$$

(3) Repeat steps (1)-(2) with baseline signal L_t as the original signal; then, the original signal X_t is decomposed into

$$X_t = \xi X_t + HX_t = \left(H\sum_{k=0}^{p-1}\xi^k + \xi^p\right)X_t, \tag{4}$$

where $H\xi^k X_t$ is the $k+1$ component of proper rotations (PRs) and $\xi^p X_t$ is the monotone trend signal. According to the above equation, the first PR component $H_t^1 = X_t - L_t^1$ can be obtained. Then, L_t^1 is decomposed until the new signal is generated, L_t^p is monotone function or constant function, and then the decomposition is stopped. The time domain and frequency domain waveform of fault signals of the rolling bearing is shown in Figure 1.

It easy can be seen from the above ITD decomposition process that the baseline signal L_t is obtained through the linear transformation of the signal, so the calculation process of ITD can be greatly simplified and the decomposition speed greatly improved.

3. AR-MED Filter

3.1. AR Filter. AR filtering is a parametric modeling method based on the rational transfer function. Because the system parameters of the AR filter are very sensitive to the state change of the system, it is of great value to apply it to signal analysis.

When the data sequence slides along the signal sequence, the adaptive AR spectrum of the signal is formed. The parameter estimation of signal sequence AR model is to select appropriate parameters so that the residual of the AR model ε_k is white noise. The commonly used methods are time series theory method and optimization theory estimation method. If there is a time series x_n, there is a positive integer p, which makes

$${}^{p}\Gamma_{x_n} = a_p, \quad (n > p), \tag{5}$$

where Γ is the Wold decomposition operator; p is analysis order; a_p is AR model parameter.

The AR model of signal sequence x_n can be expressed as

$$Y_k = \sum_{i=1}^{p} a_i x_{i+k} + \varepsilon_k, \tag{6}$$

where ε_k is a white noise process, and its variance represents the estimation error of the AR filter.

The process of linear predictive filtering using the AR filter is shown in Figure 2. After the original signal passes through p-order AR linear filter for predictive filtering, a new signal Y_n is obtained. Due to the convolution operation

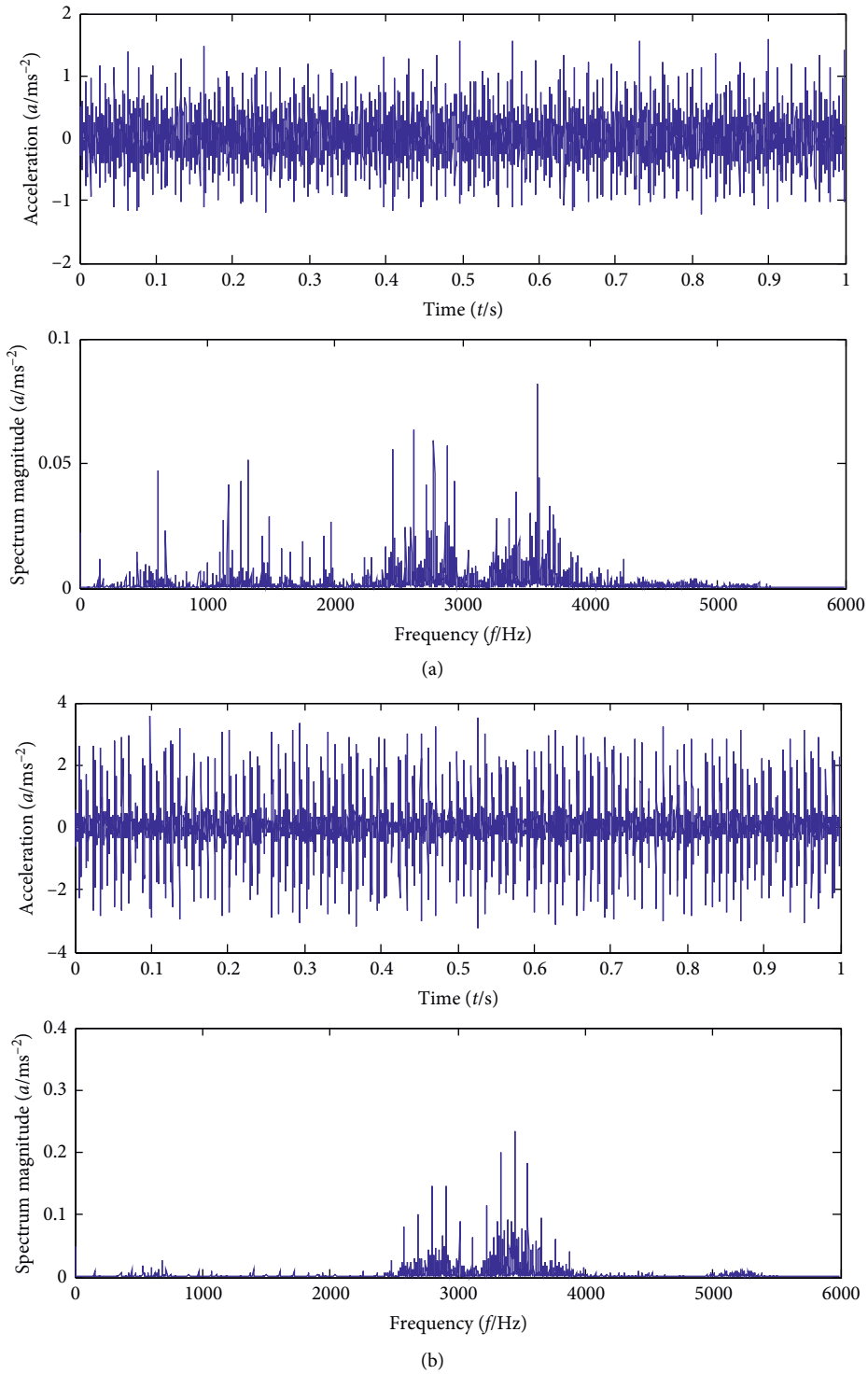

Figure 1: Time domain and frequency domain waveform of rolling bearing vibration signal: (a) inner race (IR) fault of rolling bearing vibration signal and (b) outer race (OR) fault of rolling bearing vibration signal.

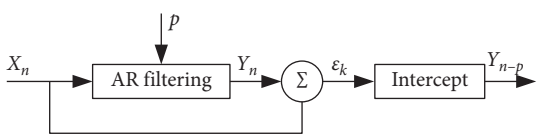

Figure 2: AR filtering process diagram.

in the filtering process, Y_n is also intercepted to obtain a signal Y_{n-p}.

3.2. MED Method. The purpose of MED is to find the source of impact in the signal. The principle is to select an appropriate filter coefficient to construct an inverse filter so that the output signal is restored to the input after the inverse filter. The minimum entropy of the signal is used as the determination condition, which can significantly improve the signal-to-noise ratio (SNR) of pulse impact signals, which is very suitable for bearing crack fault diagnosis. The fault vibration signal generated by the bearing in the event of failure usually has impact characteristics. The MED can be applied to the noise reduction treatment of impact fault of the rolling bearing to better highlight the impact pulse. It is assumed that when impact failure occurs to the rolling bearing, the collected discrete signals can be expressed as follows:

$$y_t = (g_t + n_t) * h_t, \tag{7}$$

where g_t is the signal of rolling bearing fault impact source after AR filtering; n_t is noise interference; $*$ is the convolution operator; and h_t is the influence of the transfer path.

The purpose of deconvolution is to find the filter coefficient f of the inverse filter so that the output signal y_t is restored to the input signal g_t; that is,

$$e_t = f_n * y_t = \sum_{l=1}^{L} f(l) y(n-l), \tag{8}$$

where e_t is the output signal of the inverse filter and the input signal g_t can be recovered. L is the filter length.

In this paper, the objective function method is selected to realize the MED, and the optimal inverse filter coefficient is found so that the objective function is maximized. The objective function can be defined as

$$O_4(f_l) = \frac{\sum_{n=1}^{N} e_t^2}{\left[\sum_{n=1}^{N} e_t^2\right]^2}. \tag{9}$$

Take the derivative of the objective function and set it equal to 0 to obtain

$$\frac{\partial(O_4(f_l))}{\partial(f_l)} = 0. \tag{10}$$

Since $\partial e_t / \partial f_l = y(n-l)$, we can get

$$\left[\frac{\sum_{n=1}^{N} e_t^2}{\sum_{n=1}^{N} e_t^4}\right] \sum_{n=1}^{N} e_t^3 y(n-l) = \sum_{p=1}^{L} f(p) \sum_{n=1}^{N} y(n-l) y(n-p). \tag{11}$$

Equation (11) can be written as matrix

$$f = A^{-1} b, \tag{12}$$

where b is the cross-correlation matrix of input signal g_t and output signal e_t of the inverse filter; A is Toeplitz autocorrelation matrix of inverse filter input signal g_t; and f is the filtering coefficient of the inverse filter. The solution process of MED is as follows:

(1) Toeplitz autocorrelation matrix A is calculated, and the filtering coefficient $f^{(0)}$ of the inverse filter is initialized, which is usually set as the delayed pulse.

(2) According to the initial filter coefficient $f^{(0)}$ and the inverse filter input signal $g^{(0)}$, the output signal $e^{(0)}$ is calculated.

(3) Vector $b^{(1)}$ is calculated based on the output signal $e^{(0)}$ and the input signal $g^{(0)}$.

(4) According to equation (12), $f^{(1)} = A^{-1} b^{(0)}$.

(5) Calculate the iteration error:

$$\begin{cases} \delta = \dfrac{\left(f^{(1)} - \mu f^{(0)}\right)}{\mu f^{(0)}}, \\ \mu = \dfrac{\left(E\left(f^{(0)}\right)\right)^2}{\left(E\left(f^{(1)}\right)^2\right)^{1/2}}. \end{cases} \tag{13}$$

When the expected value of the iteration error is greater than the set error threshold, that is, $E(\delta) > \tau$, $f^{(0)} = f^{(1)}$, recalculate step (2), repeat the calculation until $E(\delta) \le \tau$ or $E(\delta)$ diverges, stop the calculation, and get the MED FIR filter parameters.

4. Early Weak Fault Feature Frequency Enhance Method of Rolling Bearing Based on ITD-AR-MED

In order to enhance the feature frequency in the complex background noise, a fault feature extraction method of the rolling bearing based on the ITD-AR-MED is proposed in this paper. The flow chart of fault feature frequency enhance method of rolling bearing based on ITD-AR-MED algorithm is shown in Figure 3.

The steps of the ITD-AR-MED algorithm are as follows:

(1) Firstly, the early weak fault vibration signal of rolling bearing, which decomposed by the ITD algorithm into several PRs.

(2) Then, the sample entropy value of each PR is solved, and the PRs with the maximum entropy value is selected for subsequent processing.

(3) Finally, the selected PRs are filtered by the AR-MED method to obtain the final signal.

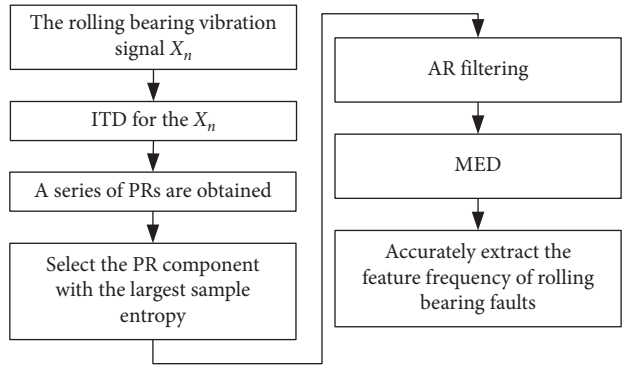

Figure 3: The flow chart of fault feature frequency enhance method of rolling bearing based on the ITD-AR-MED algorithm.

The ITD-AR-MED algorithm decomposition advantages are compared by the fast kurtogram algorithm. The simulation signals are decomposed by the ITD-AR-MED algorithm and fast kurtogram algorithm, respectively. Its simulation signal is

$$\begin{cases} x_1(t) = 0.5\cos(2\pi\omega_1 t)\cdot\cos\left(2\pi\omega_2 t + \sin\left(15\pi t^2\right)\right), \\ x_2(t) = 0.25\cos(2\pi\omega_3 t)\cdot e^{-2t^2}, \\ n(t) = \text{noise}, \\ x(t) = x_1(t) + x_2(t) + n(t), \end{cases} \tag{14}$$

where $\omega_1 = 6$, $\omega_2 = 50$, $\omega_3 = 20$, $n(t)$ is Gaussian white noise signal, t is time, $x_1(t)$, $x_2(t)$ is simulation fault signal. The time domain and frequency domain waveform of the simulation fault signal $x(t)$ is shown in Figure 4. The feature frequency of the fault simulation signal $x(t)$ is $f_1 = \omega_2 - \omega_1 = 50 - 6 = 44$ Hz, $f_2 = \omega_2 + \omega_1 = 50 + 6 = 56$ Hz, and $f_3 = \omega_3 = 20$ Hz. Time domain waveform of simulation signal $x(t)$ and its components is shown in Figure 5. Time domain waveform of ITD decomposition of simulation signals $x(t)$ and its PRs.

It can be seen from Figures 5 and 6 that the ITD algorithm can roughly decompose the component signal of the simulation signal $x(t)$.

5. Experiment Analysis

5.1. Fault Diagnosis of the Rolling Bearing Experiment. The standard rolling bearing data set selected from Case Western Reserve University (CWRU) was tested by the ITD-AR-MED method for fault diagnosis of bearing outer and inner rings [40]. The test rig is shown in Figure 7. The test rig equipment consists of motor, power meter, torque sensor, acceleration sensor, and electronic control equipment. Among them, the fault bearing should be as close as possible to the motor. The single point of bearing fault is processed by Electric Discharge Machining (EDM) technology, with a diameter of 0.117 mm and a depth of 0.011 mm. The fault vibration signal generated by the test rig is collected by the acceleration sensor, which is installed directly above the motor drive end shell. The motor frequency is 30 Hz, and the 16-channel DAT data acquisition system is adopted to collect the vibration signal of the rolling bearing fault. The signal sampling frequency is 12 kHz, the spindle speed is 1797 r/min, and the rolling bearing model is 6205-2rs JEM SKF.

According to the empirical equations (15) and (16), the fault feature frequency is 107.3 Hz and 162.2 Hz of the inner race (IR) and the outer race (OR):

$$f_0 = \frac{Z}{2}\left(1 - \frac{d}{D}\cos\alpha\right)\frac{N}{60}, \tag{15}$$

$$f_1 = \frac{Z}{2}\left(1 + \frac{d}{D}\cos\alpha\right)\frac{N}{60}, \tag{16}$$

where D is the section bearing diameter; N is the spindle speed; d is the diameter of the roll; and z is the number of the ball.

It is necessary to conduct noise reduction decomposition base on Figure 1's results. The decomposition results of the ITD algorithm for the IR fault signal and OR fault signal of the rolling bearing are shown in Figures 8 and 9, respectively.

It can be seen from Figures 8 and 9 that the IR fault signal of rolling bearing has the widest frequency range of PR1 after ITD decomposition, so it covers the most characteristic information. The OR fault signal of rolling bearing has the widest frequency range of PR2 after ITD decomposition, so it covers the most characteristic information.

The sample entropy value of each PR is obtained. Table 1 shows the sample entropy values of each PR of the rolling bearing.

According to the obtained sample entropy value of each PR component, the fault vibration signal of the IR is decomposed by the ITD, and the PR1 component is selected for subsequent analysis. After the fault vibration signal of the OR is decomposed by ITD, the PR2 component is selected for subsequent analysis.

Firstly, the PR1 of the IR fault is filtered by AR, and Figure 10 is obtained. Figure 10 shows the spectrum of the PR1 component filtered by ITD-AR. After AR filtering, the

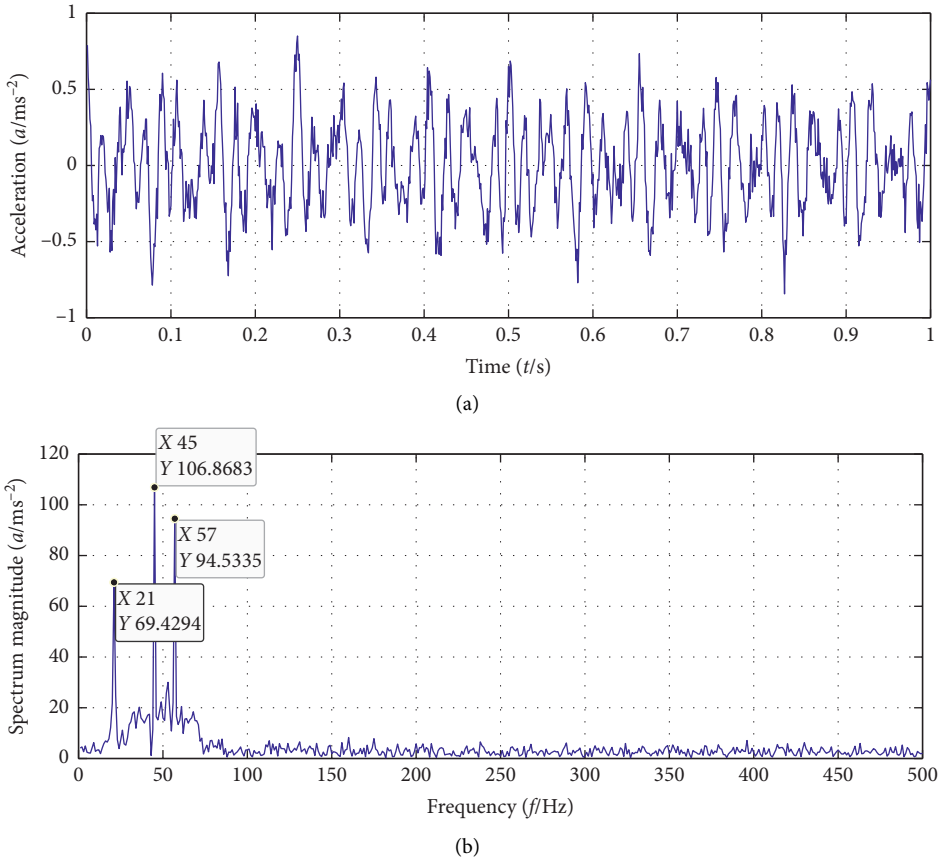

Figure 4: Time domain and frequency domain waveform of the simulation signal.

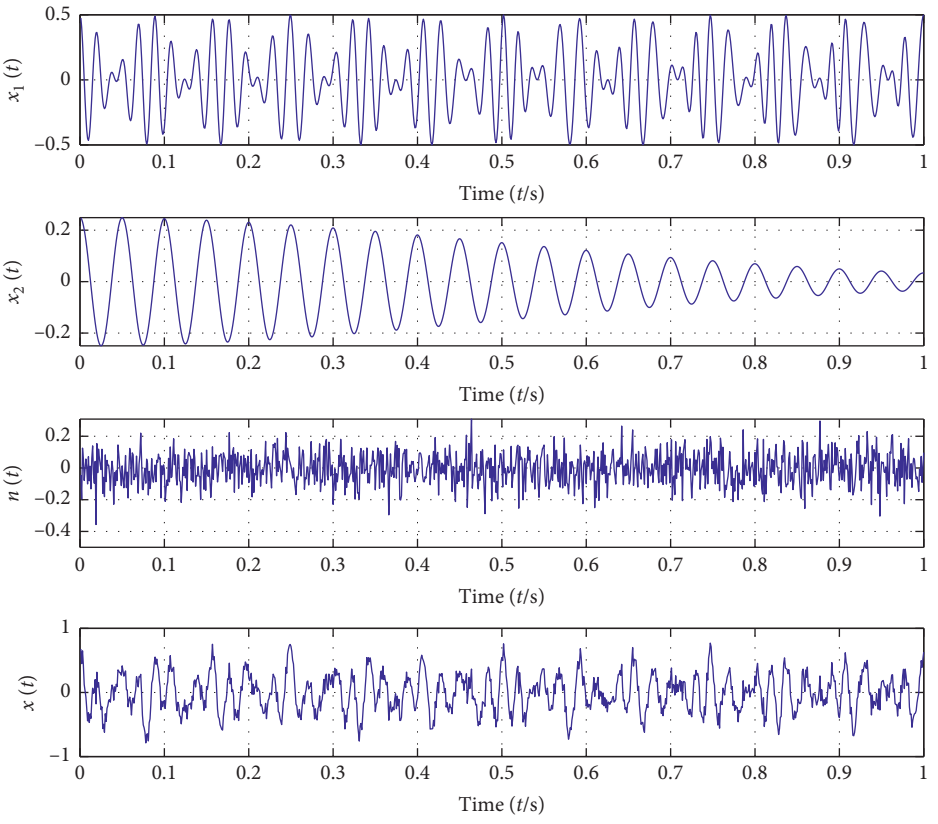

Figure 5: Time domain waveform of simulation signal $x(t)$ and its components.

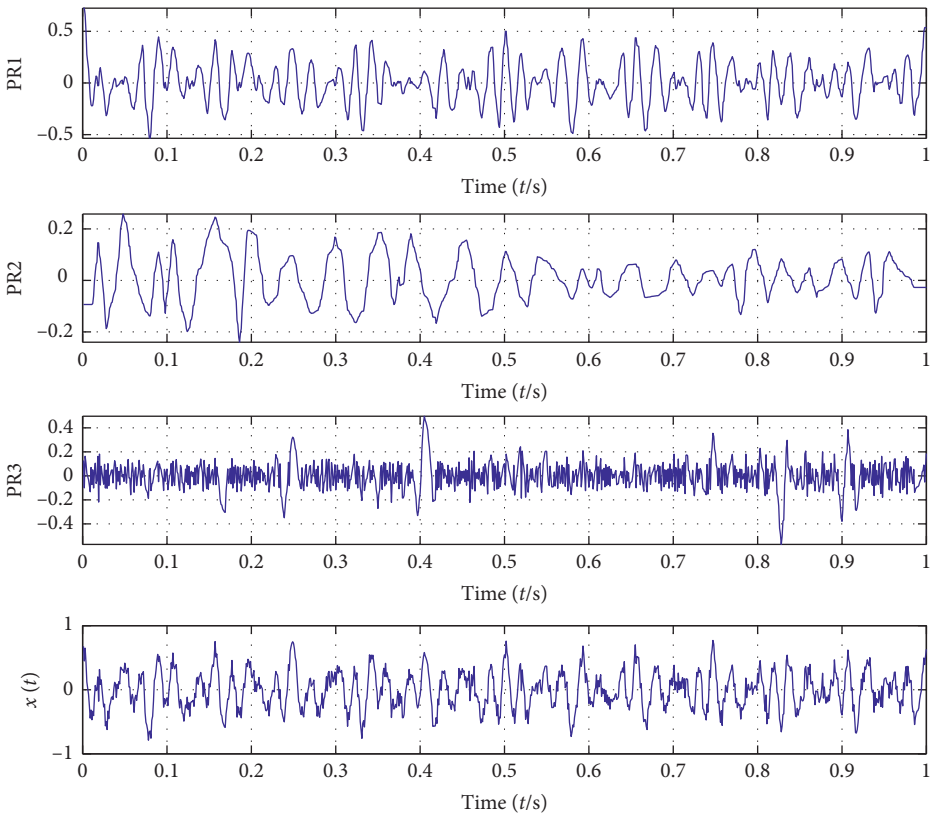

Figure 6: Time domain waveform of ITD decomposition of simulation signals $x(t)$ and its PRs.

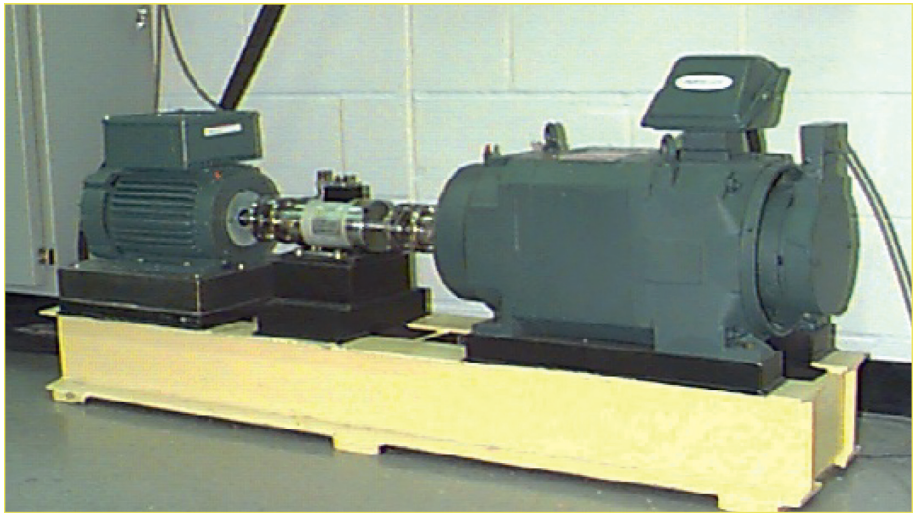

Figure 7: Test rig of the CWRU.

signal is processed by MED. Figure 11 shows the spectrum diagram of the PR1 component by the ITD-AR-MED algorithm.

Figures 10 and 11 show that the feature frequency of the IR fault vibration signal is 162.2 Hz. The envelope spectrum of PR1 by the ITD-AR-MED algorithm is shown in Figure 12.

As shown in Figure 12, the fault frequency of the PR1 can be accurately obtained, which is close to the theoretical value of 161.9 Hz. In addition, the envelope spectrum also

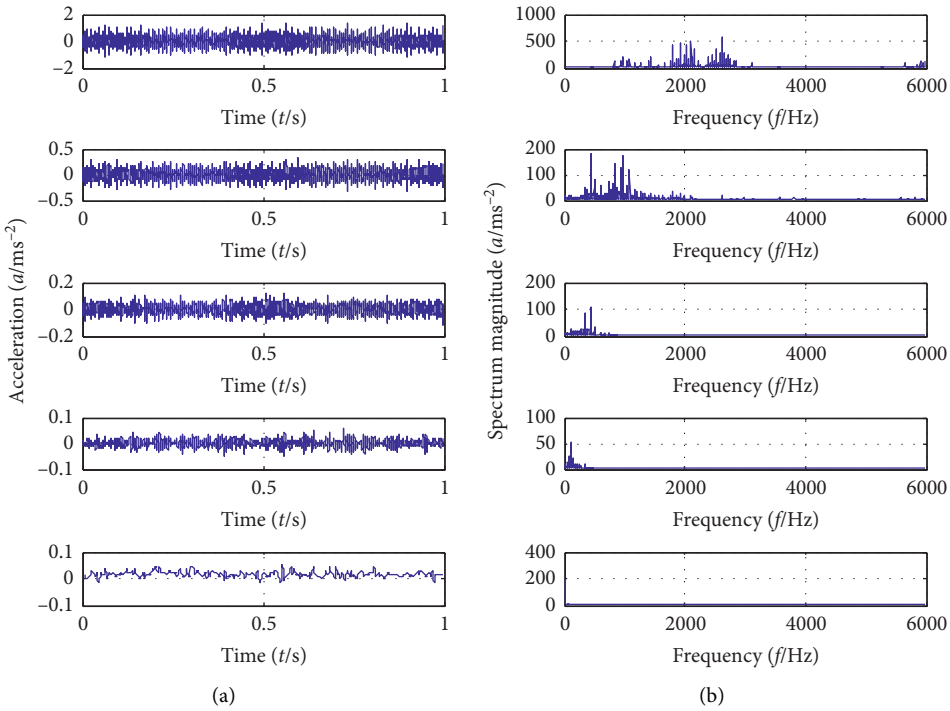

Figure 8: IR fault vibration signal of rolling bearing is decomposed by ITD.

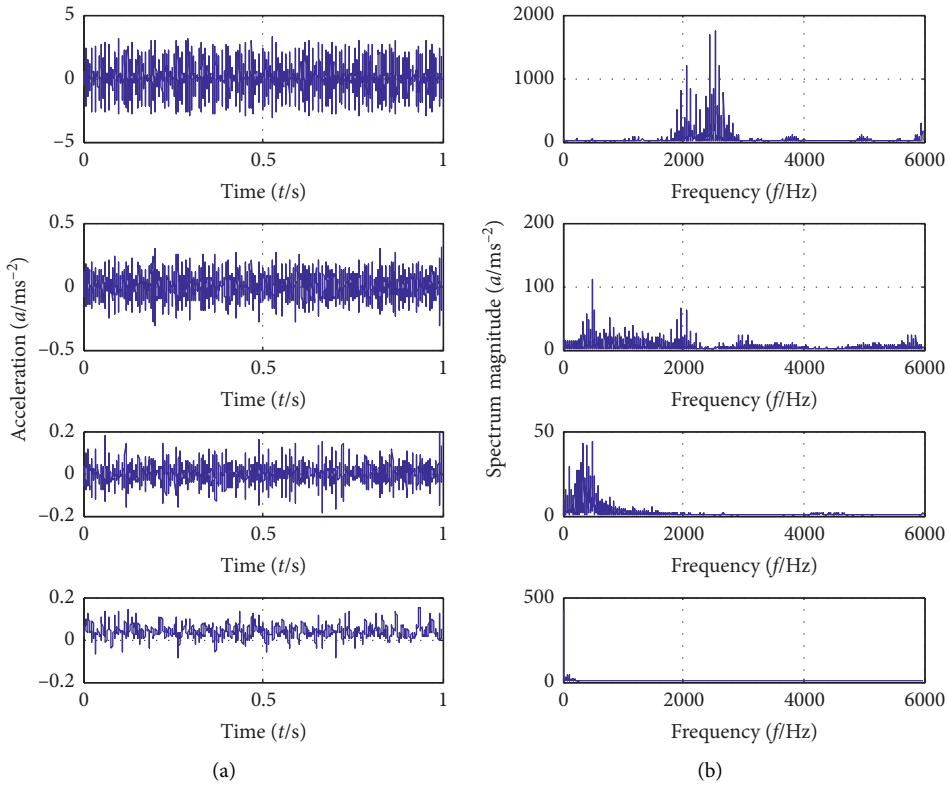

Figure 9: OR fault vibration signal of rolling bearing is decomposed by ITD.

accurately extracted the fault feature frequency at the doubling frequency of 323 Hz and the motor rotation frequency at the doubling frequency of 60.06 Hz.

Then, the fault vibration signal PR2 component is filtered by AR. The spectrum of PR2 component filtered by ITD-AR is shown in Figure 13. After AR filtering, the signal is

Table 1: Sample entropy value of each PR of IR and OR of rolling bearing.

	PR1	PR2	PR3	PR4	PR5
IR fault	1.8545	1.7907	1.2145	0.6286	0.2009
OR fault	0.9054	1.6289	0.9147	0.4052	—

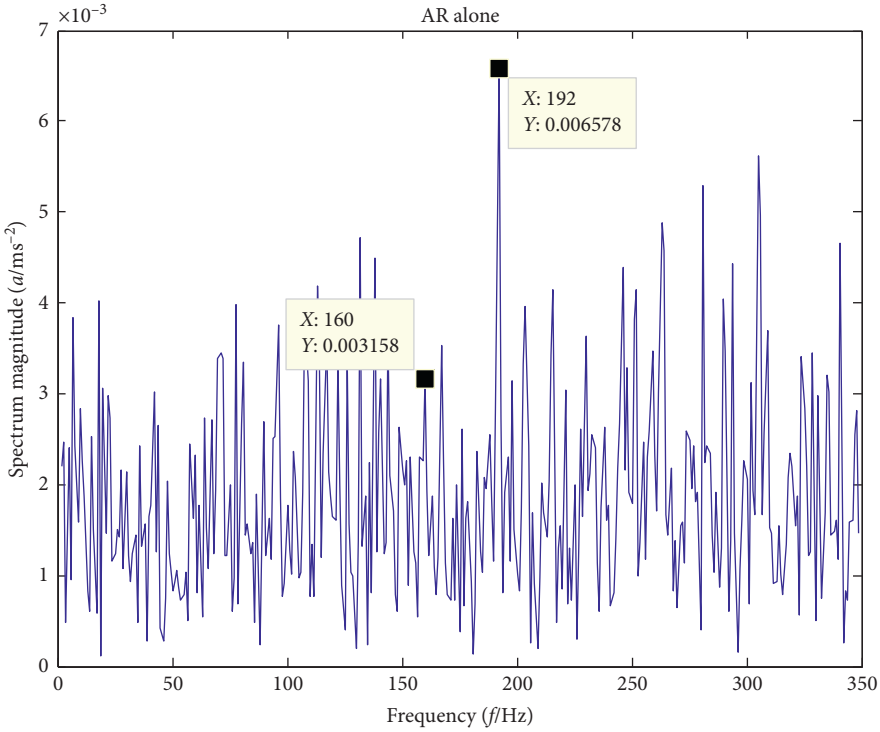

Figure 10: Spectrum diagram of PR1 component of fault vibration signal of the inner ring of rolling bearing filtered by ITD-AR.

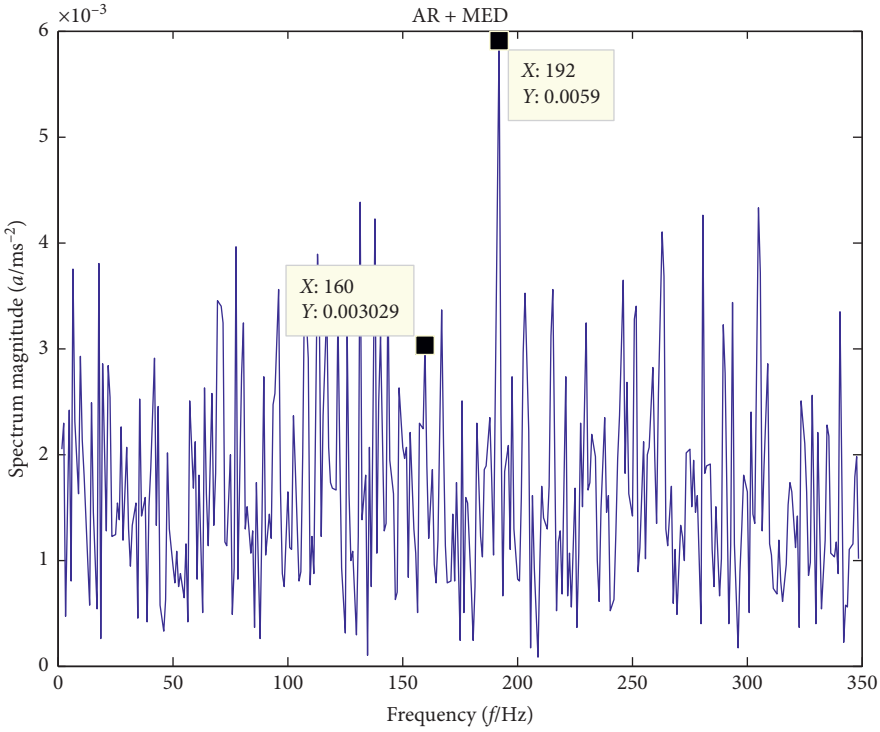

Figure 11: Spectrum diagram of PR1 component of fault vibration signal of IR of rolling bearing by ITD-AR-MED algorithm.

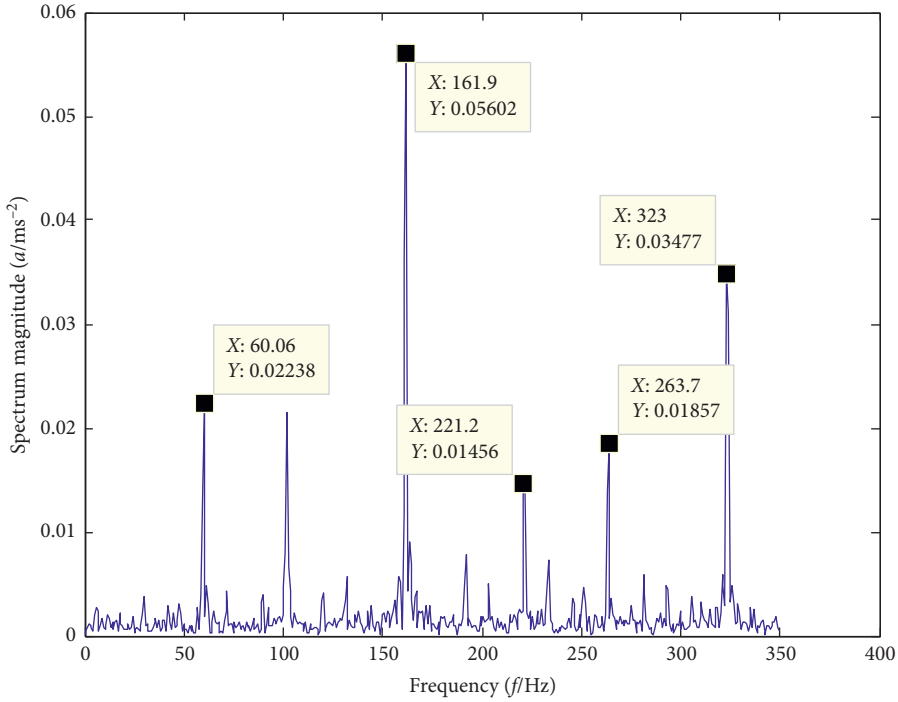

Figure 12: Envelope spectrum of fault vibration signal PR1 of IR of rolling bearing by ITD-AR-MED algorithm.

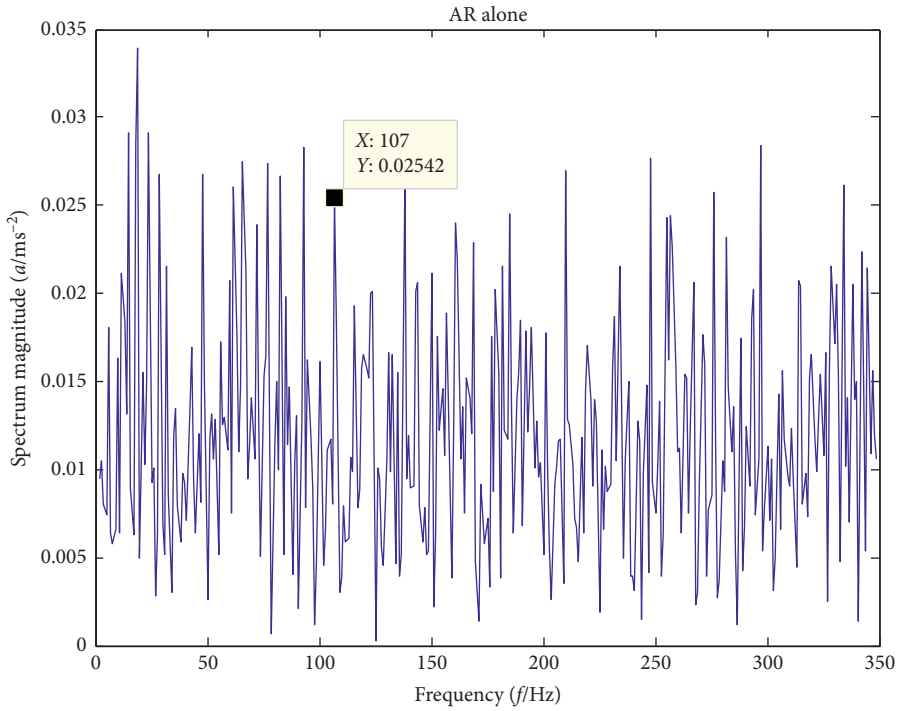

Figure 13: Spectrum diagram of PR2 component of fault vibration signal of OR of rolling bearing filtered by ITD-AR.

processed by MED. Figure 14 shows the spectrum diagram of PR2 component filtered by ITD-AR.

As shown in Figures 13 and 14, the spectrum diagram shows that the fault feature frequency is not clearly displayed at 107 Hz, which covers a large amount of background noise frequency. Therefore, the spectrum diagram obtained by the MED is used for envelope spectrum analysis. The envelope spectrum of PR2 by the ITD-AR-MED algorithm is shown in Figure 15.

As shown in Figure 15, the fault frequency of the PR2 component can be accurately obtained, which is similar to the theoretical value 107.7 Hz. In addition, the envelope

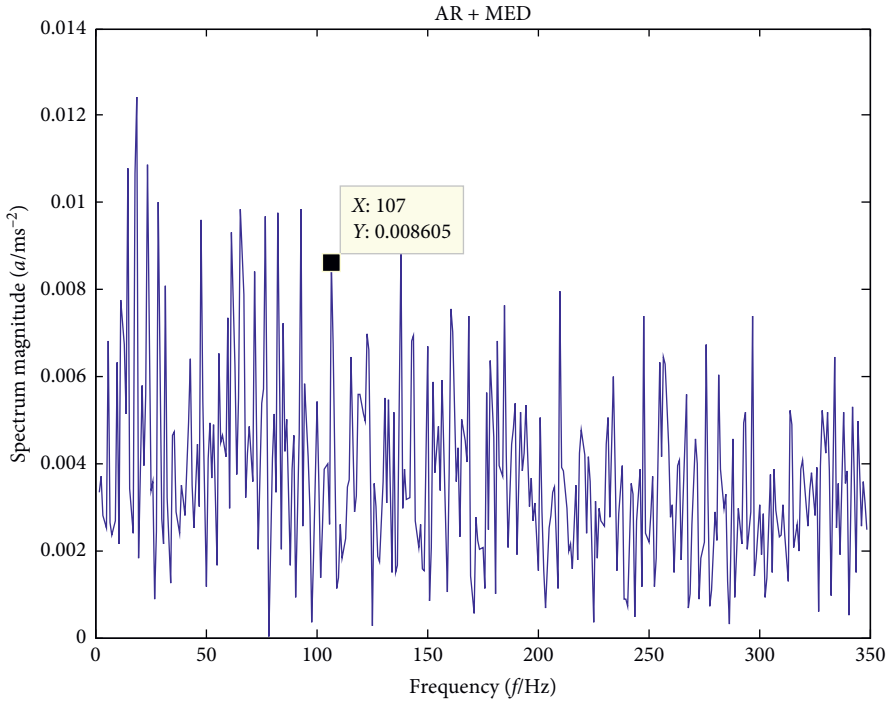

Figure 14: Spectrum diagram of PR2 component of fault vibration signal of OR of rolling bearing by ITD-AR-MED algorithm.

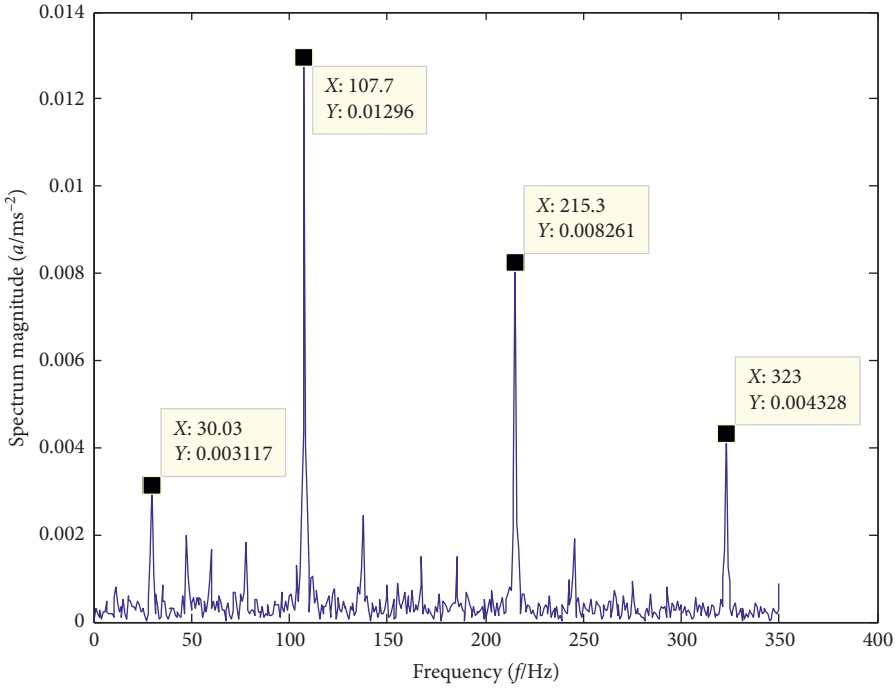

Figure 15: Envelope spectrum of fault vibration signal PR2 of OR of rolling bearing by the ITD-AR-MED algorithm.

spectrum also accurately extracted the fault feature frequency, both 215.3 Hz and 323 Hz, which are two-time frequency and three-time frequency, as well as the motor rotation frequency 30 Hz. This proves the effectiveness of the proposed fault diagnosis method.

In order to highlight the advantages of the ITD-AR-MED algorithm, the fast kurtogram algorithm is substituted for the ITD algorithm to obtain the envelope spectrum. The fault vibration signal is filtered and enhanced by the fast kurtogram algorithm. Figure 16 shows the fast kurtosis

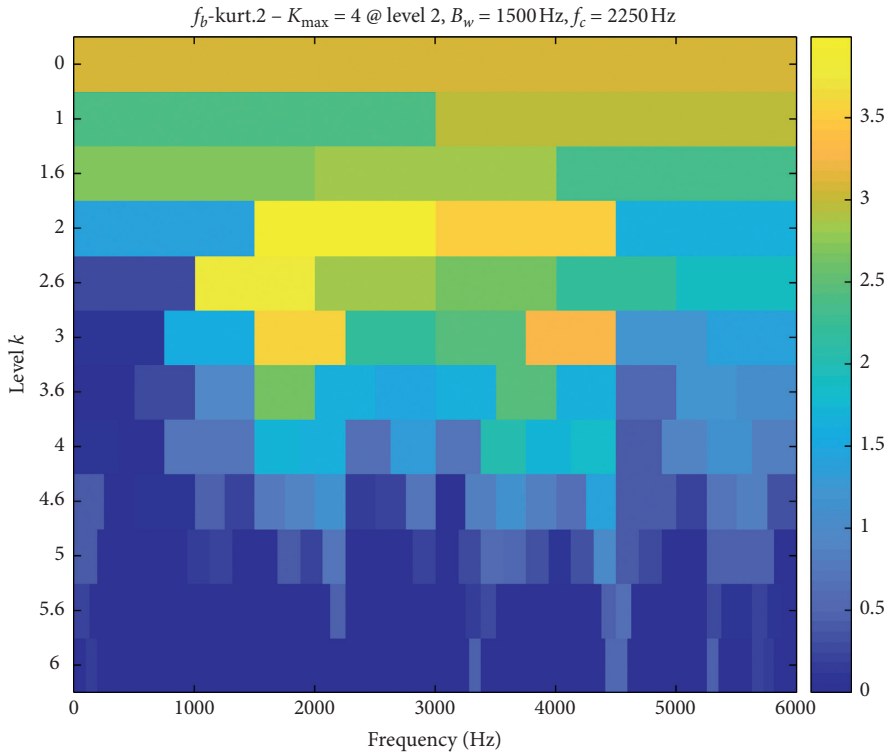

Figure 16: Fast kurtosis spectrum of rolling bearing IR fault vibration signal.

spectrum of rolling bearing IR fault vibration signal. It can be seen from Figure 16 that the IR bearing fault signal is obtained by the fast kurtogram algorithm and the center frequency and bandwidth of the bandpass filter are 2250 Hz and 1500 Hz, respectively. Figure 17 shows the envelope spectrum of the rolling bearing IR fault vibration signal after the fast kurtogram algorithm. By comparing Figure 12 with Figure 17, the fast kurtogram algorithm can extract IR fault feature frequency, but its accuracy is slightly lower than that of the ITD-AR-MED algorithm.

Figure 18 shows the fast kurtosis spectrum of rolling bearing OR fault vibration signal. It can be seen from Figure 18 that the OR bearing fault signal is obtained by the fast kurtogram algorithm and the center frequency and bandwidth of the bandpass filter are 3000 Hz and 2000 Hz, respectively. Figure 19 shows the envelope spectrum of the rolling bearing OR fault vibration signal after the fast kurtogram algorithm. By comparing Figure 15 with Figure 19, the fast kurtogram algorithm can extract OR fault feature frequency, but its accuracy is slightly lower than that of the ITD-AR-MED algorithm.

5.2. Fault Diagnosis of the Desulfurization Fan Rolling Bearing Experiment. The desulfurization fan rolling bearing test rig is shown in Figure 20. The test rig equipment consists of motor, bearing, hydraulic coupler, acceleration sensor, and fan. The signal sampling frequency is 25.6 kHz. The OR fault feature frequency is 60.31 Hz of the desulfurization fan rolling bearing.

The decomposition results of the ITD algorithm for the OR fault signal of the desulfurization fan rolling bearing are shown in Figure 21.

It can be seen from Figure 21 that the OR fault signal of the desulfurization fan rolling bearing has the widest frequency range of PR2 after ITD decomposition, so it covers the most characteristic information.

The sample entropy value of each PR is obtained. Table 2 shows the sample entropy values of each PR of the desulfurization fan rolling bearing.

According to the obtained sample entropy value of each PR component, the fault vibration signal of the OR is decomposed by the ITD, and PR2 component is selected for subsequent analysis.

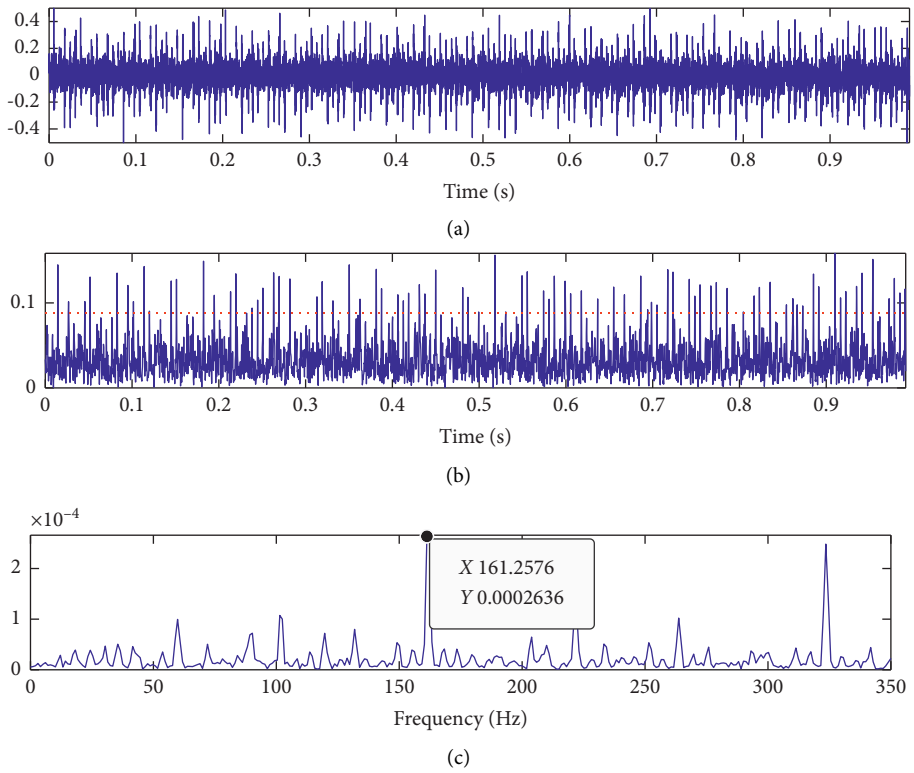

FIGURE 17: Envelope spectrum of the rolling bearing IR fault vibration signal after the fast kurtogram algorithm, (a) original signal, (b) envelope of filtered signal $B_w = F_s/2^3$, $f_c = 750$ Hz, Kurt = 1.4, $\alpha = 0.1\%$, and (c) amplitude spectrum of the squared envelope.

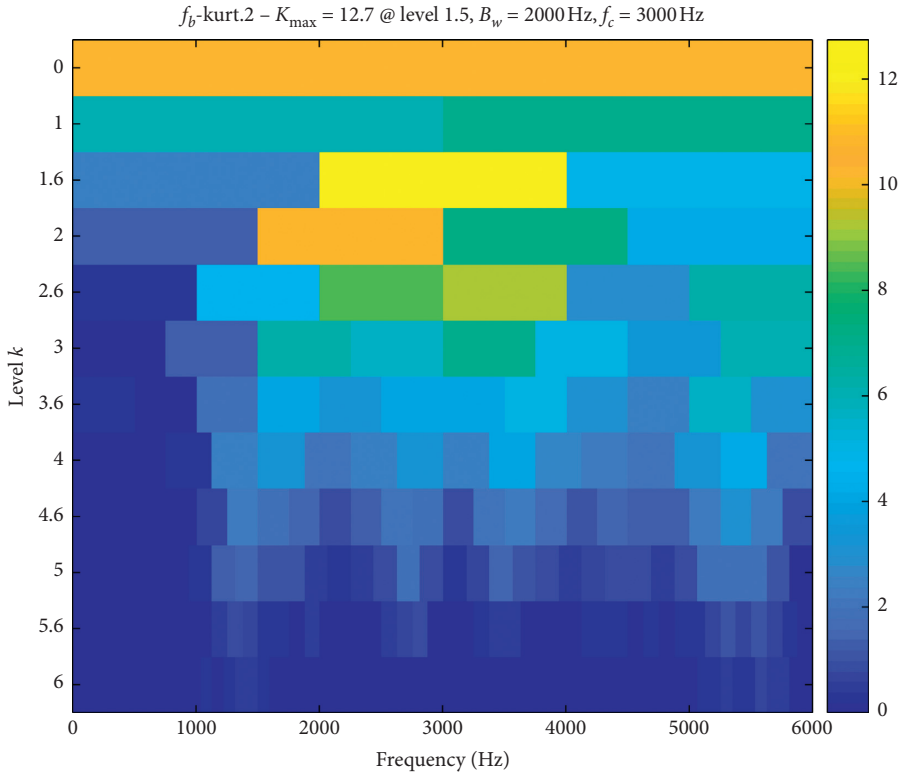

FIGURE 18: Fast kurtosis spectrum of rolling bearing OR fault vibration signal.

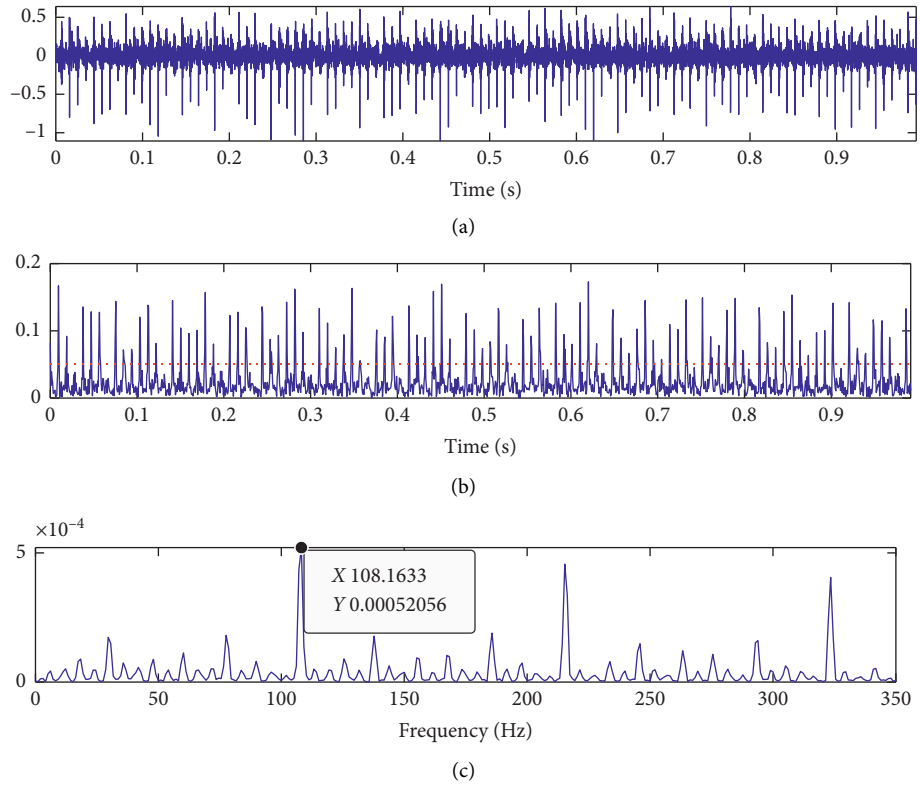

Figure 19: Envelope spectrum of the rolling bearing OR fault vibration signal after the fast kurtogram algorithm, (a) original signal, (b) envelope of filtered signal $B_w = F_s/2^4$, $f_c = 2625$ Hz, Kurt = 5.6, $\alpha = 0.1\%$, and (c) amplitude spectrum of the squared envelope.

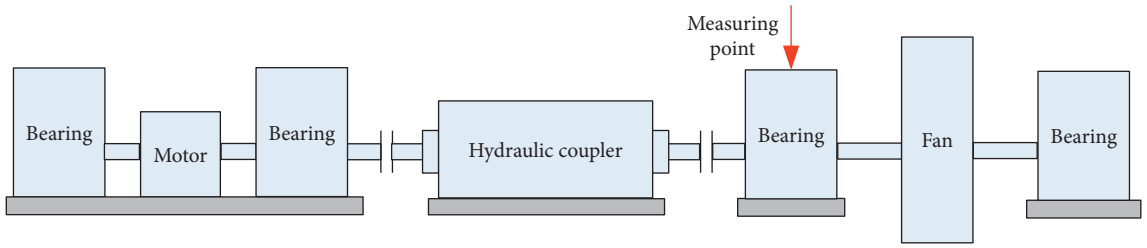

Figure 20: Test rig of the desulfurization fan rolling bearing.

Firstly, the PR2 of the IR fault is filtered by AR, and Figure 22 is obtained. Figure 22 shows the spectrum of the PR2 component filtered by ITD-AR. After AR filtering, the signal is processed by MED. Figure 23 shows the spectrum diagram of the PR2 component by the ITD-AR-MED algorithm.

Figures 22 and 23 show that the feature frequency of the OR fault vibration signal is 50 Hz. The envelope spectrum of PR1 by the ITD-AR-MED algorithm is shown in Figure 24.

As shown in Figure 24, the fault frequency of the PR2 can be accurately obtained, which is close to the theoretical value of 60.31 Hz. Figure 25 shows the fast kurtosis spectrum of the desulfurization fan rolling bearing OR fault vibration signal. It can be seen from Figure 25 that the OR bearing fault signal is obtained by the fast kurtogram algorithm and the center frequency and bandwidth of the bandpass filter are 3000 Hz and 2000 Hz, respectively. Figure 26 shows the envelope spectrum of the rolling bearing OR fault vibration signal after the fast kurtogram

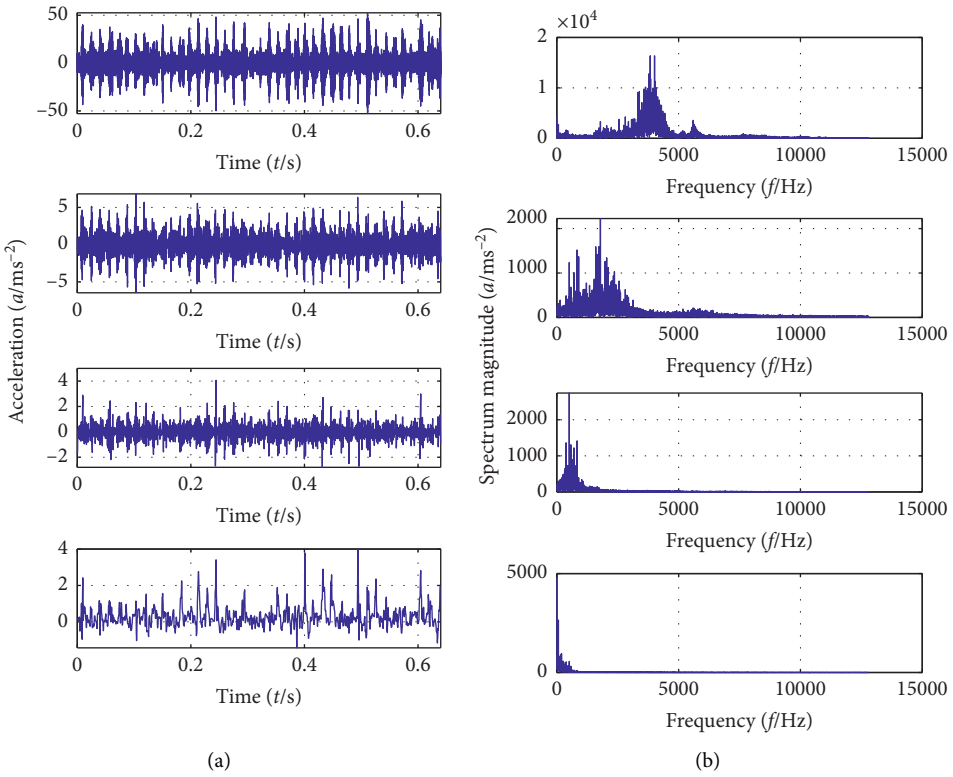

Figure 21: OR fault vibration signal of the desulfurization fan rolling bearing is decomposed by ITD.

Table 2: Sample entropy value of each PR OR fault signal of the desulfurization fan rolling bearing.

	PR1	PR2	PR3	PR4
OR fault	1.0109	1.2076	0.7348	0.2199

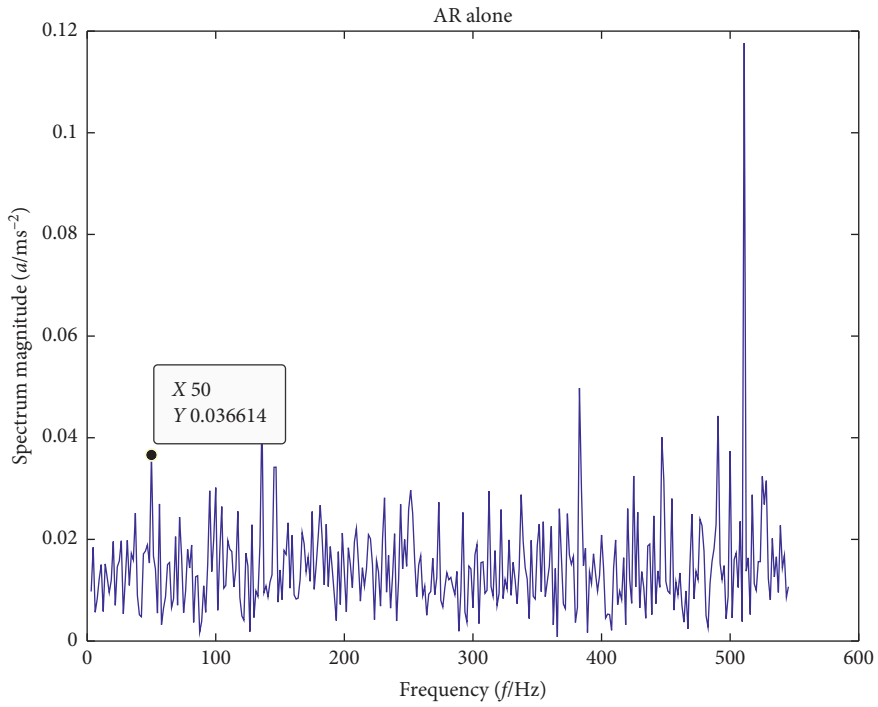

Figure 22: Spectrum diagram of the PR2 component of fault vibration signal of OR of the desulfurization fan rolling bearing filtered by ITD-AR.

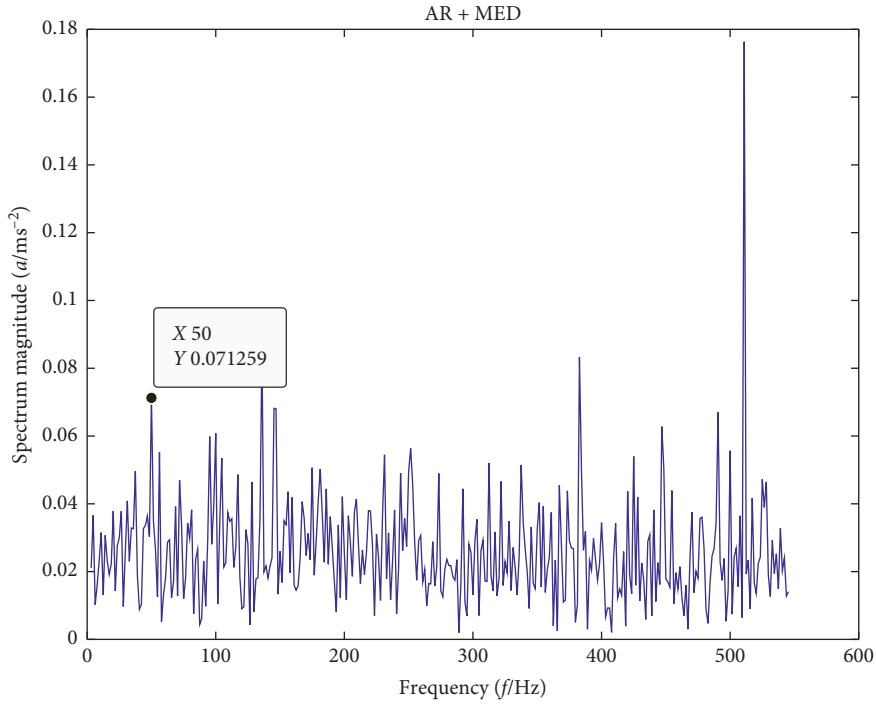

Figure 23: Spectrum diagram of the PR2 component of fault vibration signal of OR of the desulfurization fan rolling bearing by ITD-AR-MED algorithm.

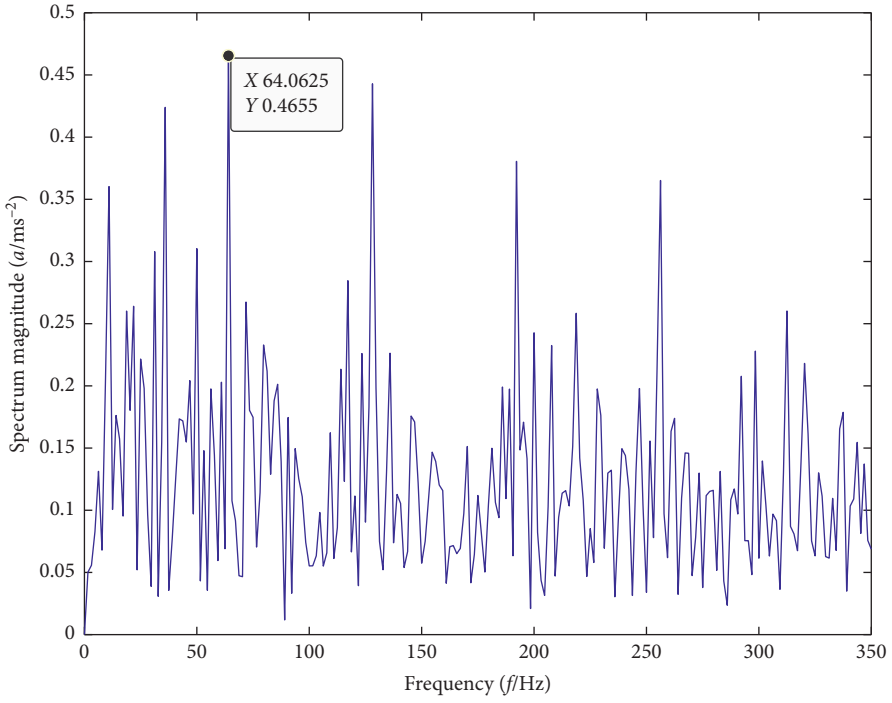

Figure 24: Envelope spectrum of fault vibration signal PR2 of OR of the desulfurization fan rolling bearing by ITD-AR-MED algorithm.

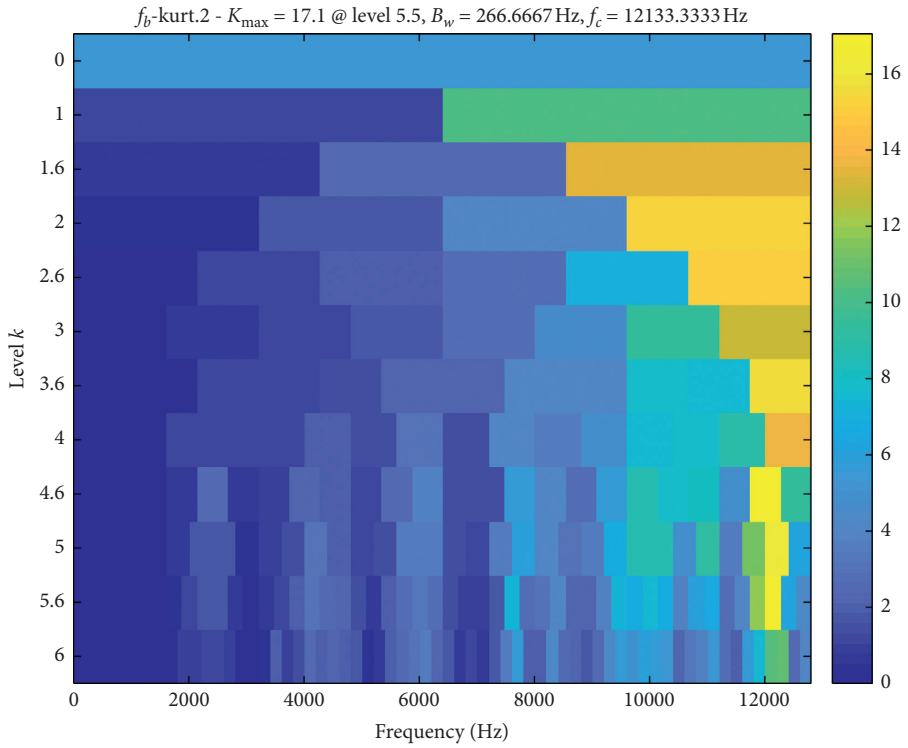

Figure 25: Fast kurtosis spectrum of the desulfurization fan rolling bearing OR fault vibration signal.

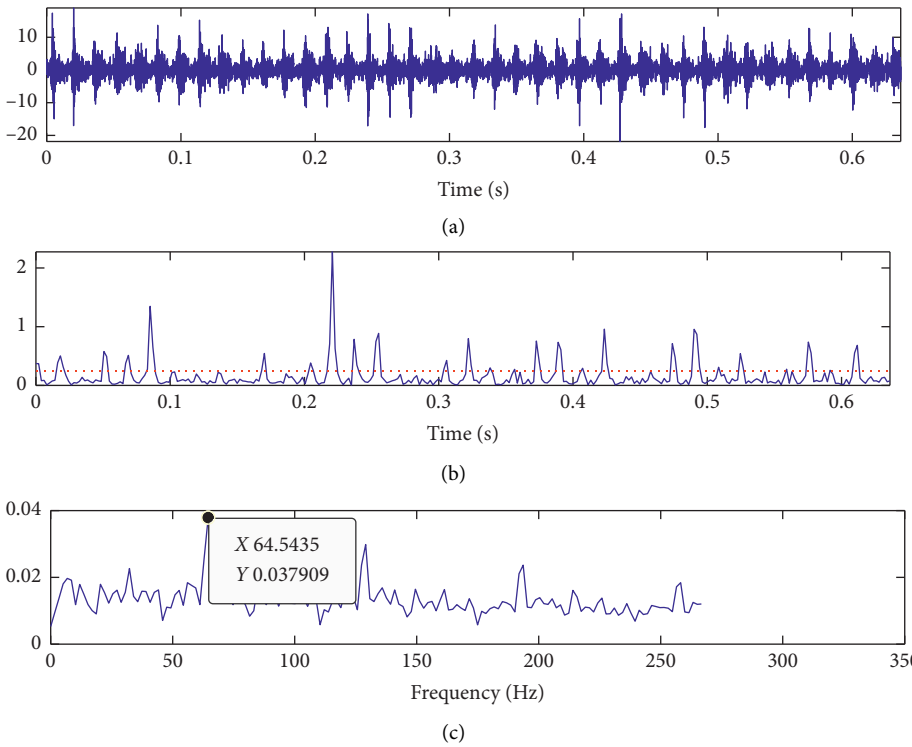

Figure 26: Envelope spectrum of the desulfurization fan rolling bearing OR fault vibration signal after the fast kurtogram algorithm, (a) original signal, (b) envelope of filtered signal $B_w = F_s/2^{6.585}$, f_c = 12133.3333 Hz, Kurt = 17.8, α = 0.1%, and (c) amplitude spectrum of the squared envelope.

algorithm. By comparing Figure 24 with Figure 26, the fast kurtogram algorithm can extract OR fault feature frequency, but its accuracy is slightly lower than that of the ITD-AR-MED algorithm.

6. Conclusions

Aiming at the difficulty of extracting the early weak fault feature frequency, the characteristics of the shock waveform of the IR and OR of rolling bearing are combined. In this paper, the ITD-AR-MED method is used for weak fault feature extraction, and the following conclusions are as follows.

(1) The ITD algorithm can decompose the early weak fault vibration signal effectively, retaining the fault impact characteristics of the rolling bearing.

(2) The MED algorithm can be used to separate the noise from the original signal. The envelope spectrum can extract the early weak fault feature frequency of the rolling bearing, which verifies the effectiveness and accuracy of the method.

Data Availability

The data used to support the findings of this study are available from the corresponding author upon request.

Conflicts of Interest

The authors declare that there are no conflicts of interest regarding the publication of this paper.

Acknowledgments

This work was cosupported by National Natural Science Foundation of China (Grant nos. 51875195 and 52075163) and National Key R&D Program of China (2020YFB2007800).

References

[1] P. Gloeckner and F.-J. Ebert, "Micro-sliding in high-speed aircraft engine ball bearings," *Tribology Transactions*, vol. 53, no. 3, pp. 369–375, 2010.

[2] H. Cao, L. Niu, S. Xi, and X. Chen, "Mechanical model development of rolling bearing-rotor systems: a review," *Mechanical Systems and Signal Processing*, vol. 102, pp. 37–58, 2018.

[3] B. L. Averbach and E. N. Bamberger, "Analysis of bearing incidents in aircraft gas turbine mainshaft bearings," *Tribology Transactions*, vol. 34, no. 2, pp. 241–247, 1991.

[4] F. Chengwei, L. Haotian, Z. Zhengzheng, A. Liqiang, L. Shaolin, and L. Cheng, "Whole-process design and experimental validation of landing gear lower drag stay with global/local linked driven optimization strategy," *Chinese Journal of Aeronautics*, 2020.

[5] C.-W. Fei, H. Li, H.-T. Liu et al., "Enhanced network learning model with intelligent operator for the motion reliability evaluation of flexible mechanism," *Aerospace Science and Technology*, vol. 107, Article ID 106342, 2020.

[6] J. Chen, J. Pan, Z. Li, Y. Zi, and X. Chen, "Generator bearing fault diagnosis for wind turbine via empirical wavelet transform using measured vibration signals," *Renewable Energy*, vol. 89, pp. 80–92, 2016.

[7] A. Kusiak and A. Verma, "Analyzing bearing faults in wind turbines: a data-mining approach," *Renewable Energy*, vol. 48, pp. 110–116, 2012.

[8] H. D. M. De Azevedo, A. M. Araújo, and N. Bouchonneau, "A review of wind turbine bearing condition monitoring: state of the art and challenges," *Renewable and Sustainable Energy Reviews*, vol. 56, pp. 368–379, 2016.

[9] X. Gong and W. Qiao, "Bearing fault diagnosis for direct-drive wind turbines via current-demodulated signals," *IEEE Transactions on Industrial Electronics*, vol. 60, no. 8, pp. 3419–3428, 2013.

[10] C. Lu, Y.-W. Feng, C.-W. Fei, and S.-Q. Bu, "Improved decomposed-coordinated kriging modeling strategy for dynamic probabilistic analysis of multicomponent structures," *IEEE Transactions on Reliability*, vol. 69, no. 2, 2020.

[11] C.-W. Fei, H. Li, H.-T. Liu, C. Lu, B. Keshtegar, and L.-Q. An, "Multilevel nested reliability-based design optimization with hybrid intelligent regression for operating assembly relationship," *Aerospace Science and Technology*, vol. 103, Article ID 105906, 2020.

[12] R. Liu, B. Yang, E. Zio, and X. Chen, "Artificial intelligence for fault diagnosis of rotating machinery: a review," *Mechanical Systems and Signal Processing*, vol. 108, pp. 33–47, 2018.

[13] J. Dybała and R. Zimroz, "Rolling bearing diagnosing method based on empirical mode decomposition of machine vibration signal," *Applied Acoustics*, vol. 77, pp. 195–203, 2014.

[14] I. Antoniadis and G. Glossiotis, "Cyclostationary analysis of rolling-element bearing vibration signals," *Journal of Sound and Vibration*, vol. 248, no. 5, pp. 829–845, 2001.

[15] S. Janjarasjitt, H. Ocak, and K. Loparo, "Bearing condition diagnosis and prognosis using applied nonlinear dynamical analysis of machine vibration signal," *Journal of Sound and Vibration*, vol. 317, no. 1-2, pp. 112–126, 2008.

[16] W. Guo and P. W. Tse, "A novel signal compression method based on optimal ensemble empirical mode decomposition for bearing vibration signals," *Journal of Sound and Vibration*, vol. 332, no. 2, pp. 423–441, 2013.

[17] H. Darong, K. Lanyan, M. Bo, Z. Ling, and S. Guoxi, "A new incipient fault diagnosis method combining improved RLS and LMD algorithm for rolling bearings with strong background noise," *IEEE Access*, vol. 6, pp. 26001–26010, 2018.

[18] J. B. Ali, N. Fnaiech, L. Saidi, B. Chebel-Morello, and F. Fnaiech, "Application of empirical mode decomposition and artificial neural network for automatic bearing fault diagnosis based on vibration signals," *Applied Acoustics*, vol. 89, pp. 16–27, 2015.

[19] L. Saidi, J. B. Ali, and F. Fnaiech, "Bi-spectrum based-EMD applied to the non-stationary vibration signals for bearing faults diagnosis," *ISA Transactions*, vol. 53, no. 5, pp. 1650–1660, 2014.

[20] H. Ocak, K. A. Loparo, and F. M. Discenzo, "Online tracking of bearing wear using wavelet packet decomposition and probabilistic modeling: a method for bearing prognostics," *Journal of Sound and Vibration*, vol. 302, no. 4-5, pp. 951–961, 2007.

[21] L.-S. Law, J. H. Kim, W. Y. H. Liew, and S.-K. Lee, "An approach based on wavelet packet decomposition and Hilbert-Huang transform (WPD-HHT) for spindle bearings condition monitoring," *Mechanical Systems and Signal Processing*, vol. 33, pp. 197–211, 2012.

[22] S. Haidong, C. Junsheng, J. Hongkai, Y. Yu, and W. Zhantao, "Enhanced deep gated recurrent unit and complex wavelet packet energy moment entropy for early fault prognosis of bearing," *Knowledge-Based Systems*, vol. 185, Article ID 105022, 2020.

[23] Y. Tian, J. Ma, C. Lu, and Z. Wang, "Rolling bearing fault diagnosis under variable conditions using LMD-SVD and extreme learning machine," *Mechanism and Machine Theory*, vol. 90, pp. 175–186, 2015.

[24] M. Han and J. Pan, "A fault diagnosis method combined with LMD, sample entropy and energy ratio for roller bearings," *Measurement*, vol. 76, pp. 7–19, 2015.

[25] W. Y. Liu, Q. W. Gao, G. Ye, R. Ma, X. N. Lu, and J. G. Han, "A novel wind turbine bearing fault diagnosis method based on Integral Extension LMD," *Measurement*, vol. 74, pp. 70–77, 2015.

[26] W.-C. Shen, Y.-H. Chen, and A.-Y. Wu, "Low-complexity sinusoidal-assisted EMD (SAEMD) algorithms for solving mode-mixing problems in HHT," *Digital Signal Processing*, vol. 24, pp. 170–186, 2014.

[27] B. Tang, S. Dong, and T. Song, "Method for eliminating mode mixing of empirical mode decomposition based on the revised blind source separation," *Signal Processing*, vol. 92, no. 1, pp. 248–258, 2012.

[28] J. Zheng, J. Cheng, and Y. Yang, "Partly ensemble empirical mode decomposition: an improved noise-assisted method for eliminating mode mixing," *Signal Processing*, vol. 96, pp. 362–374, 2014.

[29] L. Zhang, Z. Wang, and L. Quan, "Research on weak fault extraction method for alleviating the mode mixing of LMD," *Entropy*, vol. 20, no. 5, p. 387, 2018.

[30] M. G. Frei and I. Osorio, "Intrinsic time-scale decomposition: time–frequency–energy analysis and real-time filtering of non-stationary signals," *Proceedings of the Royal Society A: Mathematical, Physical and Engineering Sciences*, vol. 463, no. 2078, pp. 321–342, 2007.

[31] Z. Xing, J. Qu, Y. Chai, Q. Tang, and Y. Zhou, "Gear fault diagnosis under variable conditions with intrinsic time-scale decomposition-singular value decomposition and support vector machine," *Journal of Mechanical Science and Technology*, vol. 31, no. 2, pp. 545–553, 2017.

[32] X. An and D. Jiang, "Bearing fault diagnosis of wind turbine based on intrinsic time-scale decomposition frequency spectrum," *Proceedings of the Institution of Mechanical Engineers, Part O: Journal of Risk and Reliability*, vol. 228, no. 6, pp. 558–566, 2014.

[33] Z. Feng, X. Lin, and M. J. Zuo, "Joint amplitude and frequency demodulation analysis based on intrinsic time-scale decomposition for planetary gearbox fault diagnosis," *Mechanical Systems and Signal Processing*, vol. 72-73, pp. 223–240, 2016.

[34] L. Zhen, H. Zhengjia, Z. Yanyang, and C. Xuefeng, "Bearing condition monitoring based on shock pulse method and improved redundant lifting scheme," *Mathematics and Computers in Simulation*, vol. 79, no. 3, pp. 318–338, 2008.

[35] R. A. Wiggins, "Minimum entropy deconvolution," *Geoexploration*, vol. 16, no. 1-2, pp. 21–35, 1978.

[36] N. Sawalhi, R. B. Randall, and H. Endo, "The enhancement of fault detection and diagnosis in rolling element bearings using minimum entropy deconvolution combined with spectral kurtosis," *Mechanical Systems and Signal Processing*, vol. 21, no. 6, pp. 2616–2633, 2007.

[37] H. Endo and R. B. Randall, "Enhancement of autoregressive model based gear tooth fault detection technique by the use of minimum entropy deconvolution filter," *Mechanical Systems and Signal Processing*, vol. 21, no. 2, pp. 906–919, 2007.

[38] R. Jiang, J. Chen, G. Dong, T. Liu, and W. Xiao, "The weak fault diagnosis and condition monitoring of rolling element bearing using minimum entropy deconvolution and envelop spectrum," *Proceedings of the Institution of Mechanical Engineers, Part C: Journal of Mechanical Engineering Science*, vol. 227, no. 5, pp. 1116–1129, 2013.

[39] Q. Li, X. Ji, and S. Y. Liang, "Incipient fault feature extraction for rotating machinery based on improved AR-minimum entropy deconvolution combined with variational mode decomposition approach," *Entropy*, vol. 19, no. 7, p. 317, 2017.

[40] http://csegroups.case.edu/bearingdatacenter/pages/download-data-file.